

ACTIVE MEDIA

PACS numbers: 42.70.Hj; 42.65.Ky; 42.55.Rz
DOI: 10.1070/QE2008v038n04ABEH013575

BaY_2F_8 single crystals doped with rare-earth ions as promising up-conversion media for UV and VUV lasers*

A.A. Pushkar', T.V. Uvarova, V.N. Molchanov

***Abstract*. BaY_2F_8 crystals are studied as promising active media for UV and VUV lasers. The up-conversion pumping of rare-earth activators is proposed to solve problems related to the solarisation of the medium and the selection of pump sources. The technology of growing oriented BaY_2F_8 single crystals is developed and the influence of the crystal orientation on the growth rate and quality of single crystals is determined.**

Keywords: *BaY_2F_8, single crystal fluorides, 5d–4f transitions in rear-earth ions, UV spectral range, UV lasers.*

1. Introduction

The development of new laser transition schemes for emission in new spectral ranges is one of the important problems of quantum electronics. Solid-state laser media operating on the 5d – 4f transitions in rare-earth ions doped into wide-gap dielectric crystals are promising for the fabrication of lasers emitting in a broad UV – VUV wavelength range by using various combinations of host crystals with rare-earth ions.

At present the development of solid-state lasers of this type is mainly impeded, first, by the limited number of solid-state lasers that can be used for direct excitation of lasing at the 5d – 4f transitions in rare-earth ions and, second, by solarisation processes appearing upon direct pumping of media and leading to their degradation.

Solarisation occurs due to the absorption of pump radiation or own radiation by rare-earth ions in the excited state. As a result, electrons undergo transitions to the conduction band and are captured by neighbouring anion vacancies to form colour centres.

*Reported at the International Conference on Laser Optics (St. Petersburg, Russia, June 2006).

A.A. Pushkar', T.V. Uvarova A.M. Prokhorov General Physics Institute, Russian Academy of Sciences, ul. Vavilova 38, 119991 Moscow; Russia; e-mail: raiden.pub@gmail.com, ouvarova@ran.gpi.ru;
V.N. Molchanov A.V. Shubnikov Institute of Crystallography, Russian Academy of Sciences, Leninsky prosp., 59, 119991 Moscow, Russia

Received 14 February 2007; revision received 16 May 2007
Kvantovaya Elektronika **38** (4) 333 – 337 (2008)
Translated by M.N. Sapozhnikov

The use of up-conversion excitation schemes can solve both these problems: to avoid or considerably reduce solarisation and to find other (except neodymium lasers) pump sources such as, for example, semiconductor lasers for the development of all-solid-state UV and VUV lasers. We considered the possibility of up-conversion excitation of rare-earth ions in a monoclinic BaY_2F_8 crystal, which is a promising host crystal for the development of media of this type. The use of rare-earth ions in BaY_2F_8 crystals can provide lasing in the spectral ranges 320 – 345 nm (Ce^{3+}), 220 – 240 nm (Pr^{3+}) , 180 – 195 nm (Nd^{3+}), 165 – 170 nm (Er^{3+}), [1] and 166 – 171 nm (Tm^{3+}) because the $4f^n$ configuration of these ions has many intermediate metastable levels and they can be populated upon absorption of red and (or) IR photons emitted by available solid-state lasers.

In this paper, we demonstrate that BaY_2F_8 crystals doped with rare-earth ions are promising for up-conversion lasing in the UV and VUV spectral regions and pay special attention to the development of the manufacturing technology for these media.

2. Up-conversion excitation schemes

The up-converted VUV radiation in the range from 180 to 195 nm can be obtained in a $Nd:BaY_2F_8$ crystal by using the two-step absorption of the third-harmonic radiation from a Nd:YAG laser by Nd^{3+} ions according to the scheme presented in Fig. 1a. The first 355-nm photon excites the $^4D_{3/2}$ level of Nd^{3+} whose decay time in fluorides is a few microseconds. The second photon can excite the Nd^{3+} ion from the $^4D_{3/2}$ level to its lower d state in a BaY_2F_8 crystal. The corresponding absorption band has a maximum at 56×10^3 cm^{-1} and a half-width of 2200 cm^{-1}. The lifetime of this d state is tens of nanoseconds [1].

The lowest level of the d state is located at 27863 cm^{-1} above the $^4D_{3/2}$ level, while the 355-nm pump photon energy is 28169 cm^{-1}. The difference of these energies (306 cm^{-1}) lies within the half-width of the absorption band, sufficiently close to its maximum, and therefore up-conversion excitation of Nd ions in $Nd:BaY_2Y_8$ crystals can be performed according to the scheme in Fig. 1a if the effective absorption cross section for Nd with the atomic concentration of 0.4 % in the excited state is sufficiently large. The authors of [2] measured the effective absorption cross section for Nd in the excited $^4D_{3/2}$ state in a BaY_2F_8 crystal of unknown orientation and obtained a very low value smaller than 10^{-20} cm^2. It is possible that the

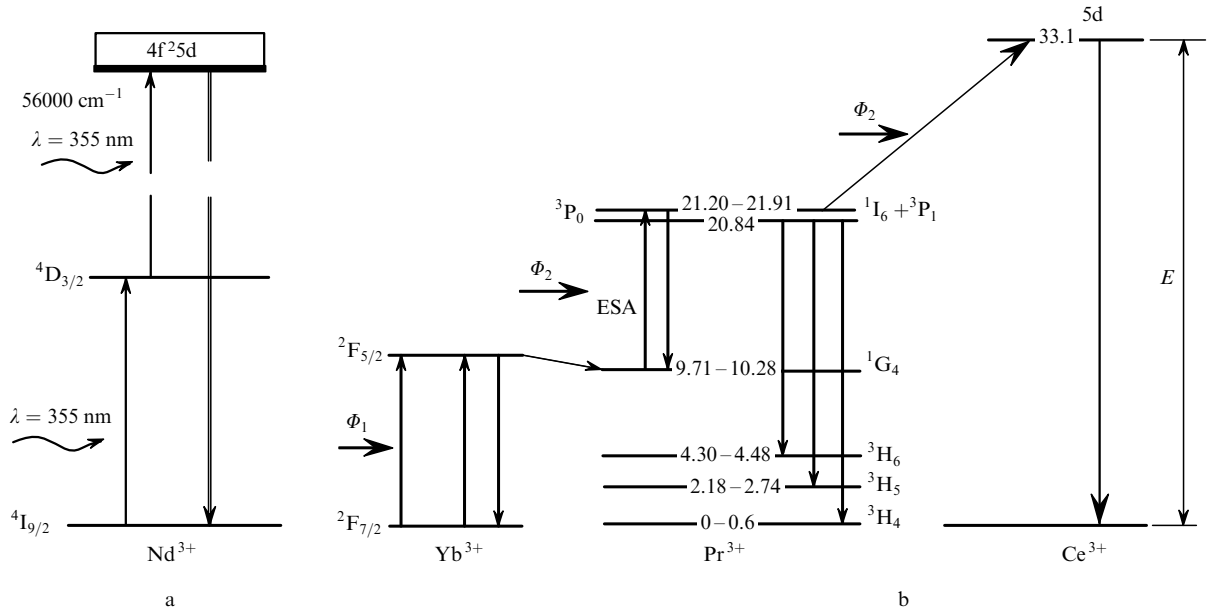

Figure 1. Schemes of up-conversion pumping of a $BaY_2F_8:Nd^{3+}$ single crystal by the third harmonic of a Nd:YAG laser (a) and up-conversion avalanche pumping of a Pr,Ce,Yb:BaY_2F_8 single crystal (b). The figures denote level energies (in 10^3 cm^{-1}).

orientation of the crystal was not optimal. We hope to determine the optimal orientation of BaY_3F_8 by studying the anisotropy of lasing and spectroscopic parameters of crystals doped with Nd at atomic concentrations from 0.2 % to 0.8 %.

The up-converted UV radiation in the range 320–345 nm can be also obtained in a Pr, Ce, Yb:BaY_2F_8 crystal according to the scheme presented in Fig. 1b.

In this case, up-conversion in governed by the avalanche mechanism based on the efficient excited-state absorption (ESA) from the intermediate $^1G_4$ level, which is called a 'sink' level. By using a strong absorption in Yb^{3+} ions in the IR region ($\sim$1 μm) and efficient energy transfer from Yb^{3+} to other rare-earth ions [3], we plan to use the combined doping of crystals with Yb^{3+}, Pr^{3+}, and Ce^{3+} ions. In this case, to achieve the efficient ion–ion interaction, the concentration of rare-earth ions should be high enough.

The lower $4f^25d$ level of Ce^{3+} is populated at several stages. The $^2F_{5/2}$ level of the Yb^{3+} ion is directly populated by exciting Yb^{3+} by a semiconductor laser diode (beam Φ_1) at the $^2F_{7/2} \rightarrow {}^2F_{5/2}$ transition. The lifetime of this level is quite large ($\sim$250μs). To provide the efficient interaction between Yb^{3+} and Pr^{3+} ions (energy exchange between the $^2F_{5/2}$ level of Yb^{3+} and the $^1G_4$ level of Pr^{3+}), these ions should be located at small enough distance from each other.

The $^1G_4$ [$^1G_4 \rightarrow (^1I_6, {}^3P_1)$] absorption of the second 800-nm pump beam Φ_2 from the excited $^1G_4$ state is accompanied by the rapid nonradiative $(^1I_6, {}^3P_1) \rightarrow {}^3P_0$ transition resulting in the population of the $^3P_0$ level. During the $(^2F_{7/2}, {}^2F_{5/2}) \rightarrow (^1G_4, {}^3P_0)$ cross relaxation, the $^3P_0$ level is pumped again, the increase in the population of the $^1G_4$ level at each stage resulting in the increase in ESA.

To populate the lower 5d level of the Ce^{3+} ion, the ion should absorb radiation of the second pump beam Φ_2 and energy transfer from the $^3P_0$ level of the Pr^{3+} ion to the 5d level of the Ce^{3+} ion should occur. As a result, it becomes possible to develop an all-solid-state UV laser with convenient IR pump sources.

Another example of using a laser diode as a pump source is the scheme of the $^4I_{9/2} \rightarrow {}^4F_{9/2}$ (Nd^{3+}) $\rightarrow$ 5d (Ce^{3+}) transition accompanied by UV lasing in the range 320–345 nm. By using co-doping of a BaY_2F_8 crystal with Nd^{3+} and Ce^{3+} ions, the lower 5d level of Ce^{3+} can be pumped by a laser diode in the region from 645 to 690 nm (the photon energy $E = 15504 - 14493$ cm^{-1}) in two stages: (i) the first photon is absorbed by the $^4F_{9/2}$ level of Nd^{3+} and (ii) the second photon populates the lower 5d level of Ce^{3+} due to ESA. The corresponding absorption band has a maximum at 33000 cm^{-1} and half-width $\sim$1600 cm^{-1}.

The co-doping of BaY_2F_8 single crystals with several rare-earth ions opens up wide possibilities for using various schemes of pumping by solid-state lasers. For example, co-doping with $Pr^{3+}$and Nd^{3+} ions allows one to perform two-step pumping of the 5d state of the Pr^{3+} ion accompanied by lasing at $\sim$217 nm: first the $^4G_{9/2} + {}^2K_{13/2}$ level (19055–20040 cm^{-1}) of the Nd^{3+} ion is populated after absorption of the first photon (the second harmonic from a Nd:YAG laser) and then the second 355-nm photon (the third harmonic from a Nd:YAG laser) populates the 5d level (46000 cm^{-1}) of the Pr^{3+} ion.

We have demonstrated the wide possibilities for the development of various up-conversion schemes based on BaY_2F_8 crystals co-doped with different rare-earth ions. In addition, we plan to select optimal concentration ratios for activators and optimal orientation of the crystal for increasing the efficiency of IR–UV energy transfer.

3. Single-crystal growth method

Single crystals were grown by the Bridgman method in a multicell graphite crucible with seed channels. A graphite heater and a system of coaxial screens provided the three-zone temperature profile consisting of an almost gradient-free melting zone, a short (50–70 °C cm^{-1}) growth zone with a strong gradient , and a long crystal cooling zone with a very low gradient (7–10 °C cm^{-1}). This thermal unit was used for growing laser crystals of length up to 100 mm

transmitting in the range from 125 nm to 10 μm. The crucible travel velocity was varied from 1.5 to 11 mm h^{-1}.

A charge was prepared from high-purity dry BaF_2 and RF_3 (R is a rare-earth ion). The mass content of transition and rare-earth impurities in them did not exceed 10^{-4} % and the oxygen content did not exceed 5×10^{-3} %. A charge of the required composition was prepared by weighting, mixing, and melting the initial components in the atmosphere of high-purity argon and products of the thermal decomposition of Teflon.

Activators were introduced in the form of melted BaR_2F_8 compositions. The BaY_2F_8 boules obtained in this way were oriented in an ENRAF – NONIUS four-circle diffractometer. Then, seeds of the specified orientation were cut out, which were used for growing many oriented pure BaY_2F_8 crystals or crystals doped with rare-earth ions [4].

4. Crystal structure and anisotropy of its properties

The binary BaR_2F_8 compounds of the stoichiometric composition are crystallised to the monoclinic syngony and belong to the $C2/_m - C^3_{2h}$ spatial group. The BaY_2F_8 crystal lattice parameters are $a = 6.972$, $b = 10.505$, $c = 4.260$, and $\beta = 99^\circ$. These are optically biaxial crystals. Their stability is determined by the size of a rare-earth polyhedron, i.e. eventually by the radius of a rare-earth ion forming a rigid three-dimensional skeleton with interstices occupied by barium ions. The positions of cations are separated, the difference between their coordination numbers being great: the coordination number of barium is 12, while that of a rare earth ion is 8. Because rare-earth activators occupy the position of Y, no charge compensation is required upon doping. The BaY_2F_8 crystals have 100 % isomorphous capacity with respect to rare-earth ions of the yttrium subgroup, excluding Lu^{3+}. This structure is not formed in systems with rare-earth ions of the cerium subgroup because a polyhedron, which increases proportionally to the ionic radius of a rare-earth ion, becomes too large for a Ba atom [5].

By using a strong anisotropy of the crystal properties along different crystallographic axes, we plan to select the optimal crystal orientation to reduce the lasing threshold and enhance the lasing efficiency. In papers [2, 5 – 8] devoted to the study of anisotropic properties of BaY_2F_8 crystals, the electrical conduction and some lasing and spectroscopic parameters of these crystals were investigated only in two directions: parallel and perpendicular to the only second-order [010] axis. Because BaY_2F_8 crystals are biaxial, the orientation of the tensors of effective cross sections with respect to the crystallographic axis can considerably change within the multiplets under study. Therefore, to characterise the anisotropy of the transitions completely, it is necessary to perform spectral measurements by changing the angle between the electric field and crystallographic axes by steps.

We have grown several series of BaY_2F_8 crystals at different crucible travel velocities and determined the properties of their growth. The predominant growth direction, which we called the *r* axis, was found to coincide with the $[11\bar{1}]$ direction. We have grown transparent BaY_2F_8 single crystals with this orientation, which had no cracks and inclusion when the crucible travel velocity was 11 mm h^{-1}, whereas we have failed to obtain crystals without cracks grown in other directions, even when the crucible velocity was only 2.8 mm h^{-1}. We explain the appearance of unpredictable stresses and cracks by a low symmetry of this crystal and strong anisotropy of its properties.

5. Introduction of activators

The BaY_2F_8 crystals have a high isomorphous capacity with respect to rare-earth ions of the yttrium subgroup; however, rare-earth ions of the cerium subgroup are non-isomorphous with respect to these crystals and have a low solubility in the solid state. In this connection the introduction of Ce^{3+}, Pr^{3+}, and Nd^{3+} activators leads to the appearance of small inclusions in the crystal volume, the inhomogeneous distribution of activators over the crystal length, stresses, and cracks. In this section, we discuss the distribution of Ce^{3+}, Pr^{3+}, and Nd^{3+} over the crystal length, the maximum entering of this activators to the BaY_2F_8 crystal lattice and the influence of Yb^{3+} ions on the entering of Ce^{3+} and Pr^{3+} ions into crystals at different growth rates. Table 1 presents the radii of free Y^{3+}, Yb^{3+}, Ce^{3+}, Pr^{3+}, and Nd^{3+} ions [9].

The ionic radius increases in a series Yb^{3+}, Y^{3+}, Nd^{3+}, Pr^{3+}, Ce^{3+}. After the introduction of cerium subgroup activators, the local size of a rare-earth polyhedron forming the skeleton of a BaY_2F_8 crystal increases, and therefore stresses in the crystal increase with increasing the activator concentration, resulting in the formation of cracks. At a certain activator concentration, the polyhedron becomes too large for the introduction of the Ba^{2+} ion, and then the formation of the second phase in the form of small inclusions is observed. The crystal defectiveness increases with the increase in the difference between the ionic radii of the activator and Y^{3+}.

Table 1. Ionic radii of Yb^{3+}, Y^{3+}, Nd^{3+}, Pr^{3+}, and Ce^{3+}.

Ion	Yb^{3+}	Y^{3+}	Nd^{3+}	Pr^{3+}	Ce^{3+}
Ionic radius/nm	0.0858	0.097	0.0995	0.1013	0.102

Figure 2 illustrates the change in the absorption coefficients for Pr^{3+} and Ce^{3+} ions along the crystal axis, which corresponds to the extrusion of these ions during the crystal growth. The spectra of Nd^{3+} did not demonstrate the activator extrusion during the crystal growth in the range of initial atomic concentrations from 0.01 % to 1 %, while at the concentration ~1 % the impurity extrusion occurred at the very beginning of the crystal.

We calculated the effective distribution coefficient K_{eff} and the limiting activator entering coefficient C_{lim} by using the Galliver – Pfann equation transformed by the method proposed in [4]:

$$C_g = K_{\text{eff}} C_0 (1 - g)^{K_{\text{eff}} - 1}, \tag{1}$$

where C_g is the activator concentration in the crystal; C_0 is the initial activator concentration; and g is the fraction of the crystallised material.

For crystals with a high activator concentration, in which the separation of the second phase was observed, the coefficient K_{eff} was calculated for two crystals grown in one series by using the Galliver – Pfann equation in the form

$$K_{\text{eff}} = \frac{\lg(C_{01}/C_{02})}{\lg(1 - g_2)/(1 - g_1)} + 1, \tag{2}$$

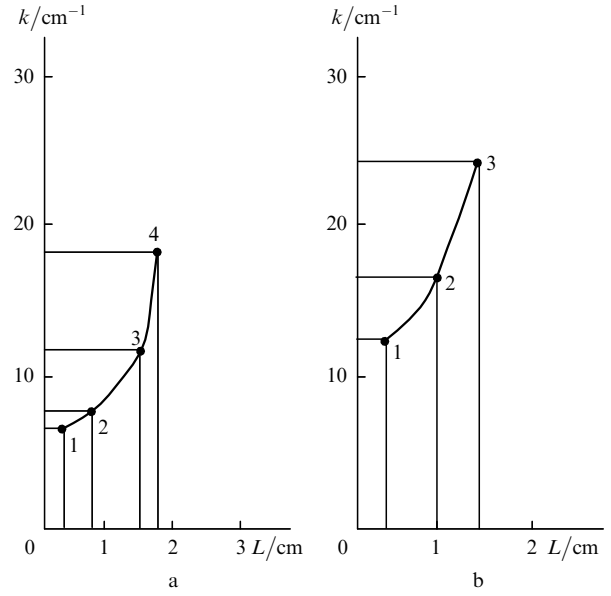

Figure 2. Change in the absorption coefficient of the Ce^{3+} ions along the growth axis L of the BaY_2F_8 crystal corresponding to the extrusion of these ions during the crystal growth (for the atomic concentration of Ce^{3+} equal to 0.113 %) (a) and change in the absorption coefficient of Pr^{3+} along the growth axis of the BaY_2F_8 crystal for the atomic concentration of Pr^{3+} equal to 0.0216 %. The measurement error is $\Delta k = 0.5$ cm^{-1}, $\Delta L = 0.1$ cm.

where C_{01} and C_{02} are the initial activator concentrations in the first and second crystals; g_1 and g_2 are the fractions of the crystallised material in each crystal at the impurity precipitation boundary.

Then, by using the obtained values of K_{eff}, we calculated from (1) the limiting entering of the activator into these crystals. The results are presented in Table 2.

Table 2. Limiting entering of C_{lim} and the effective distribution coefficients K_{eff} of Pr^{3+} и Ce^{3+} ions in a BaY_2F_8 single crystal.

Composition containing activators	V/mm h^{-1}	C_0 (%)	K_{eff}	C_{lim} (%)
$BaPr_2F_8$	2.75	0.4 – 0.8	0.89 ± 0.02	0.87 ± 0.02
$BaYb_2F_8$ + $BaPr_2F_8$	2.75	0.5 1 – 6	0.89 ± 0.02	–
$BaCe_2F_8$	2.75	0.13 – 0.951	0.78 ± 0.06	0.66 ± 0.06
$BaCe_2F_8$	2.4	0.13 – 0.951	0.52 ± 0.05	0.68 ± 0.04
$BaPr_2F_8$	1.44	0.0216	0.42 ± 0.04	–

Note: V is the crystallisation rate.

For crystals with low activator concentrations, in which the second phase was not separated, we transformed Eqn (1) in another way, by using absorption spectra (Fig. 2). Calculations were performed by using the absorption coefficients of the activator at two adjacent points of the same crystal.

If the activator concentration at the first point of the crystal is

$$C_{g_1'} = K_{\text{eff}} C_0 (1 - g_1')^{K_{\text{eff}}-1}, \tag{3}$$

and at the second point is

$$C_{g_2''} = K_{\text{eff}} C_0 (1 - g_2'')^{K_{\text{eff}}-1}, \tag{4}$$

then by dividing Eqn (3) by (4) and taking the logarithm, we obtain

$$\lg \frac{C_{g_1'}}{C_{g_2''}} = (K_{\text{eff}} - 1) \lg \frac{1 - g_1'}{1 - g_2''}. \tag{5}$$

Because the absorption coefficient K_{abs} is proportional to the activator concentration in the crystal, by substituting into (5) the ratio of absorption coefficients instead of the concentration ratio, we obtain

$$K_{\text{eff}} = \frac{\lg(K_{\text{abs}\,1}/K_{\text{abs}\,2})}{\lg[(1 - g_1')/(1 - g_2'')]} + 1. \tag{6}$$

Here, $K_{\text{abs}\,1}$ and $K_{\text{abs}\,2}$ are the absorption coefficients of the activator at points 1 and 2 of the crystal; and g_1' and g_2'' are the fractions of the crystallised material at these points, respectively.

The calculation was performed by using K_{abs} at the first three points in Fig. 2 (in pairs) because point 4 is located in fact at the end of the crystal, where the Galliver – Pfann equation becomes uncertain. The results presented in Table 2 show that the limiting entering of the activator to the BaY_2F_8 lattice decreases with increasing its ionic radius. Its value does not exceed 1 for Nd, 0.87 for Pr, and 0.68 for Ce. The coefficient K_{eff} strongly depends on the crystallisation rate, and it can be expected that the value of K_{eff} will be close to 1 already at the crystallisation rate 5 mm h^{-1}, which will provide the synthesis of crystals with the uniform distribution of the activator over the crystal length. Such rates can be used by growing pure BaY_2F_8 crystals in the direction r and b (see section 4). However, doping of crystals with Ce^{3+} or Pr^{3+} ions produces local stresses during the crystal growth at the sites of their introduction into the lattice due to the difference between the ionic radii of Y^{3+} and activators. For this reason, stresses in crystals grown at high rates (5.5 mm h^{-1}) increased with increasing concentration.

For example, cracks appeared in crystals containing Pr^{3+} at concentrations above 0.5 % in the absence of Yb^{3+}, whereas no cracks were observed in crystals co-doped with Pr^{3+} and Yb^{3+} (the Yb^{3+} concentration did not exceed 1 %) and grown at the same rate.

Because the ionic radius of Yb^{3+} is smaller than that of Y^{3+}, during the formation of $BaY_2F_8 - BaYb_2F_8$ solid solutions the averaged lattice parameter proportionally decreases compared to that for a pure BaY_2F_8 crystal, which should negatively affect the entering of Ce^{3+} and Pr^{3+}. However, if the local entering is considered, we can assume that ions of the cerium subgroup will tend to localise near ytterbium. This can be explained by the fact that ytterbium, having a smaller ionic radius, forms a polyhedron of a smaller size than yttrium, thereby releasing space for the neighbouring polyhedron into which a larger ion, for example, Pr^{3+} or Ce^{3+} can enter.

6. Conclusions

We have developed possible up-conversion excitation schemes for doped BaY_2F_0 single crystals. The oriented BaY_2F_8 single crystals doped with rare-earth ions of the

cerium subgroup have been grown by the Bridgman method. It has been shown that the homogeneous distribution of activators of the cerium subgroup can be obtained in crystals grown along the crystallographic axis *b* and in the predominant growth direction *r*.

A strong anisotropy of the growth rate and formation of defects along different crystallographic axes has been observed. The predominant growth direction has been found for BaY_2F_8 crystals (the $[11\bar{1}]$ direction *r*).

At present we continue the development of new up-conversion excitation schemes for BaY_2F_8 single crystals doped with rear-earth ions for obtaining lasing at other wavelengths in the UV – VUV region.

Acknowledgements. This work was supported by the Russian Foundation for Basic Research (Grant No. 07-02-01157).

References

1. Chernov S.P., Ivanova O.N., Uvarova T.V., et al. *Phys. Stat. Sol.*, **88**, 169 (1985).
2. Guyot Y., Guy S., Jobert M.F. *J. Alloys and Compounds*, **323–324**, 722 (2001).
3. Joubert M.F. *Opt. Mater.*, **11**, 181 (1999).
4. Uvarova T.V., Pushkar' A.A., Molchanov V.N. *Izv. Vyssh. Uchebn. Zaved., Mater. Elektron. Tekh.*, **4**, 34 (2004).
5. Trnocova V., Fedorov P.P., Bystrova A.A., et al. *Sol. State Ionics*, **106**, 301 (1998).
6. Lo D., Makhov V.N., Krupa J.C., et al. *J. Luminescence*, **106**, 15 (2004).
7. Owen J., Cheetham A., Farlane R. *J. Opt. Soc. Am. B.*, **15**, 2 (1998).
8. Owen J., Jarman R., Thrash R., et al. *J. Opt. Soc. Am. B*, **11**, 5 (1994).
9. Tkachenko N.L., Garashina L.S., Izotova O.E., et al. *J. Sol. State Chem.*, **8**, 213 (1973).